

# Average turn-over frequency of O<sub>2</sub> electro-reduction for Fe/N/C and Co/N/C catalysts in PEFCs

Frédéric Jaouen <sup>\*,1</sup>, Jean-Pol Dodelet <sup>\*,1</sup>

INRS Énergie, Matériaux et Télécommunications, 1650 Bd Lionel Boulet,  
Varennnes, Québec, Canada J3X 1S2

Received 5 January 2007; received in revised form 6 March 2007; accepted 15 March 2007  
Available online 21 March 2007

## Abstract

This work aims to evaluate the average turn-over frequency of O<sub>2</sub> electro-reduction for the catalytic sites resulting from the heat-treatment of iron- or cobalt-acetate and carbon black in ammonia at high temperature. This task is complex because at least three factors may control the activity of such catalysts: their metal content, nitrogen content and micropore specific area. In this work, the activity was measured for metal contents from 0.005 to 5 wt.%. The time of heat-treatment was tuned to keep the micropore specific area constant. At Fe content  $\leq 0.2$  wt.% the activity increases linearly with Fe content, thus enabling the average turn-over frequency of the Fe/N/C site to be determined. At Co content  $\leq 1.0$  wt.% the activity increases approximately as the square root of the Co content. Because no linear relation was found, the turn-over frequency of the Co/N/C site could not be determined. For both Fe and Co catalysts, the activity drops dramatically at contents  $>1$  wt.%. This is concurrent with a drop in the micropore specific area of the catalysts.

© 2007 Elsevier Ltd. All rights reserved.

**Keywords:** Polymer electrolyte fuel cell; Non-noble catalyst; Metal loading; Oxygen reduction

## 1. Introduction

Polymer electrolyte fuel cells (PEFCs) are an alternative to (i) internal combustion engines in the transportation market and to (ii) primary or secondary batteries in the portable electronics market. One impediment to their commercialization is the high materials cost of which the catalyst, platinum, occupies a major place. While mass production of PEFCs would result in lowered costs for bipolar plates and membranes, the Pt cost is incompressible due its scarcity [1]. Thus, it is important to either reduce the loading of Pt or Pt-group metals or replace them with non-noble catalysts. Reducing the Pt loading (in g/kW at given cell voltage) can be realized by increasing its intrinsic catalytic activity through alloying with non-noble metals such as Cr, Mn, Fe, Co or Ni [2,3] or by enhancing its utilization through the deposition of Pt monolayers on nanoparticles [4,5]

or by improving mass-transport properties of electrodes at high current density.

The present paper is concerned with the difficult task of replacing Pt by non-noble catalysts at the PEFC cathode where the oxygen reduction reaction (ORR) takes place. Several families of such catalysts for the ORR in acidic medium are under investigation today. They may be divided into two groups, either using a heat-treatment in the catalyst preparation procedure, or not. In the first group, Fe- or Co-based catalysts are obtained after heat-treating: (i) a metal-centered macrocyclic compound (porphyrin, phthalocyanine) adsorbed on a carbon support [6–9], (ii) an unsupported chelate in the presence of a foaming agent [10,11], (iii) a metal salt in the presence of carbon and nitrogen [12–24], or (iv) a sputter-deposited Fe<sub>x</sub>C<sub>1-x-y</sub>N<sub>y</sub> film [25]. In the second group, Co-based catalysts are obtained without heat-treating the Co precursor. For such procedure, Co-based catalytic sites are either obtained after plasma treatment of a carbon supported porphyrin [26] or based on the interaction of Co with polypyrrole [27]. Recent reviews covered the subject of non-noble catalysts for PEFCs [28,29]. Assuming that the above families of non-noble catalysts for the ORR are either stable or can be stabilized in PEFC environment, another important question

\* Corresponding author. Tel.: +1 450 929 8142; fax: +1 450 929 8198.

\*\* Corresponding author. Tel.: +1 450 929 8143; fax: +1 450 929 8102.

E-mail addresses: [jaouen@emt.inrs.ca](mailto:jaouen@emt.inrs.ca) (F. Jaouen),

[dodelet@emt.inrs.ca](mailto:dodelet@emt.inrs.ca) (J.-P. Dodelet).

<sup>1</sup> ISE member.

is: can these catalysts reach an activity that meets the requirement for a commercial use? Even if the cost of such non-noble catalysts is negligible compared to Pt, their acceptable level of activity cannot be orders of magnitude lower than that of Pt: the thickness of efficient cathodes in PEFCs is limited because of mass- and charge-transport limitations. Thus, the decrease in activity when switching from Pt to a non-noble catalyst must be compensated for by making the cathode thicker. If the decrease in activity is so large that it cannot be wholly compensated, this means that the materials cost (cost per kW of electricity) in membrane or bipolar plate will rise when using the non-noble catalyst. This is not acceptable from a commercial standpoint.

Gasteiger et al. set the target of ORR activity for non-noble catalysts in automotive applications as  $1/10^{\text{th}}$  of the Pt state-of-the-art activity [3]. This compromise on the activity is viable under the assumption that efficient, 100- $\mu\text{m}$  thick cathodes for non-noble catalysts (against typically 10- $\mu\text{m}$  thick for current Pt cathodes) will become feasible. Following, the target for non-noble catalysts in automotive applications according to these authors is a volumetric activity of  $130 \text{ A/cm}^3$  of electrode at 0.8 V versus SHE,  $80^\circ\text{C}$  and under an  $\text{O}_2$  absolute pressure of 1 bar (Table 6 in Ref. [3]). The previous figure ( $\text{A/cm}^3$  electrode at 0.8 V) for any catalyst is equal to the mathematical product of the site density (number of active sites/ $\text{cm}^3$ ), turn-over frequency (number of electrons reduced per active site and per second at 0.8 V) and electric charge of a single electron ( $p$ , 30 in Ref. [3]). The turn-over frequency depends on the electrochemical overpotential while the site density is a constant. It is therefore of interest to appraise as precisely as possible the turn-over frequency of such catalysts in order to predict if the above target can be reached and what practical site density it implies.

Previously, the turn-over frequency (ToF) of three non-noble catalysts has been estimated on the basis of published works [3]. However, all three estimated values are subject to large errors due to (i) the assumption of an activation energy of  $55 \text{ kJ/mol O}_2$  that was used to correct two out of three literature data measured at  $20$  or  $50^\circ\text{C}$  to the reference temperature of  $80^\circ\text{C}$  chosen by Gasteiger et al., and (ii) the assumption that all metal atoms were efficiently used in active sites for the catalysts described in the literature. For assumption (i), an error of up to a factor 10 on the turn-over frequency may incur, as noted by the authors [3]. Extrapolating an activity measured at  $20^\circ\text{C}$  to that expected at  $80^\circ\text{C}$  may lead to a decade overestimation if the true energy of activation is, e.g. 22 instead of  $55 \text{ kJ/mol O}_2$  (even for the extensively studied Pt, activation energies spanning  $22$ – $76 \text{ kJ/mol O}_2$  have been reported [30,31]). For assumption (ii), several papers have shown that the activity levels off at Fe loadings  $>0.15 \text{ wt.}\%$  (iron acetate precursor) [16,32] or  $>1 \text{ wt.}\%$  (iron porphyrin precursor) [18] for such catalysts, meaning that some of the metal atoms may not form active sites. Thus assumption (ii) could also lead to an error of a factor 10 on the turn-over frequency, e.g. in the case of a catalyst containing  $2 \text{ wt.}\%$  Fe, of which only  $0.2\%$  formed active sites. Due to the combined or separate effect of these two sources of error, it is not surprising that the turn-over frequency of three Fe-based non-noble catalysts spanned a wide range from 0.02 to 1.7 electrons per active site (i.e. per

metal atom) and per second [3]. Thus, the turn-over frequency of such catalysts, and hence their practical potential, remains unclear.

The object of this paper is thus to measure the turn-over frequency for  $\text{O}_2$  electro-reduction of Fe/N/C and Co/N/C catalytic sites obtained from a heat-treatment, and to compare it to the target set by Gasteiger et al. in well-defined experimental conditions (fuel cell,  $80^\circ\text{C}$ ,  $p_{\text{O}_2}$  1 bar, 0.8 V versus SHE). It is reminded that previous studies on Fe/N/C catalysts demonstrated that two catalytic sites are simultaneously present in such materials [33]. No such conclusion could be reached for Co/N/C catalysts [34]. Therefore, the turn-over frequency measured in this study is, for the Fe catalysts, a value averaged over the different active sites. When estimating the average turn-over frequency of such catalytic sites, it is important to investigate catalysts with low metal contents in which, presumably, all metal atoms form active sites. A last difficulty in measuring the average turn-over frequency resides in the importance of the micropore specific area of the carbon support [23]. An experimental strategy was chosen in order to maintain the micropore specific area constant, and this independently of the metal loading. The present study will first investigate, at room temperature and in sulphuric acid solution, the activity against the metal content ( $0.005$ – $5 \text{ wt.}\%$ ). It will be shown that a range of Fe content exists in which the activity increases linearly. In contrast, Co catalysts in the same range display an activity increasing only as the square root of the Co content. Thus, the turn-over frequency could be determined only for the Fe/N/C site. Then, the activity (Fe and Co) and average turn-over frequency (Fe only) are measured on carefully chosen catalysts at  $80^\circ\text{C}$  in fuel cell. From the knowledge of the average turn-over frequency at  $80^\circ\text{C}$  in PEFC, it is then possible to calculate the theoretical site density necessary to reach the target of activity ( $\text{A/cm}^3$  electrode at 0.8 V versus SHE) for non-noble catalysts for an automotive application.

## 2. Experimental

### 2.1. Catalyst synthesis (fully detailed in [23])

The furnace black (Sid Richardson Carbon Company) has a BET area of  $71 \text{ m}^2 \text{ g}^{-1}$  (micropore area  $5 \text{ m}^2 \text{ g}^{-1}$ ). It is the same furnace black than the one used in Ref. [23] and is characterized by N, O, and S contents of 0.66, 0.44, and 0.65 at.%, respectively. For targeted metal loadings  $>0.05 \text{ wt.}\%$ , metal acetate is weighed ( $m_{\text{MeAc}}$ ) and dissolved in distilled water. For targeted metal loadings  $<0.05 \text{ wt.}\%$ , the mass of metal acetate is too small to be accurately weighed and, instead, a dilute solution is prepared, from which the required aliquot is pipetted (to which corresponds a known mass of metal acetate,  $m_{\text{MeAc}}$ ). Then, if  $x$  is the mass fraction of metal (e.g.  $0.2 \text{ wt.}\%$  metal yields  $x = 2 \times 10^{-3}$ ) desired in the (carbon black + metal) powder, then the mass of carbon to weight is  $m_{\text{MeAc}}t(1-x)/x$  with  $t = 0.3212$  being the mass of iron in iron acetate; or  $t = 0.2366$  that of cobalt in cobalt acetate hydrated with four water molecules. Commonly,  $550$ – $600 \text{ mg}$  of carbon is added and dispersed in  $100$ – $120 \text{ mL}$  of the water solution containing the metal acetate.

The suspension is stirred and then dried overnight in an oven at 80 °C. About 500 mg of the resulting powder is ground and placed in a quartz boat. The exact mass before heat-treatment,  $m_i$ , is measured. The quartz boat with the powder, as well as a glass rod/interior magnet assembly, is placed in a quartz tube, but outside of the oven. The tube is first purged with argon. The oven is then switched on and allowed to stabilize at its set temperature (940 °C; corresponding to an inner-tube temperature of 950 °C) for 2 h (supplementary information of Ref. [23]). After 100 min of stabilization, the argon flow is switched to pure ammonia with a flow rate of 2000 sccm. Twenty minutes later, the boat is pushed into the middle of the oven and the chronometer is started. The heat-treatment is ended by removing the quartz tube from the oven. The powder after the heat-treatment is again weighed and yields  $m_f$ . The weight loss percentage of carbon during the heat-treatment in  $\text{NH}_3$  is

$$W = 100 \times \frac{m_i - m_f}{m_i} \quad (1)$$

This weight loss is the result of a gasification reaction of carbon black by  $\text{NH}_3$  occurring at a fast rate above 800 °C and yielding mainly HCN and  $\text{H}_2$  [35].

## 2.2. Activity and selectivity at room temperature: rotating (ring) disk electrode technique

The catalytic activity and  $\text{H}_2\text{O}_2$  yield are measured in a solution of sulphuric acid of pH one saturated by pure  $\text{O}_2$ . An ink

of the catalyst is prepared by mixing 10 mg of catalytic powder, 95  $\mu\text{L}$  of a 5 wt.% Nafion solution (Aldrich) and 350  $\mu\text{L}$  of ethanol for 30–60 min. Seven microliters of the ink are pipetted onto a glassy carbon disk (0.2  $\text{cm}^2$ ), resulting in a catalyst loading (iron plus carbon) on the glassy carbon of 0.8  $\text{mg cm}^{-1}$ . Cyclic voltammograms with a sweep rate of 10  $\text{mV s}^{-1}$  are recorded in the potential range of  $-0.25$  to  $0.75$  V versus a saturated calomel electrode (SCE). When the electrode is not rotated, in the downward potential scan, a peak reduction current occurs, owing to  $\text{O}_2$  reduction kinetics and  $\text{O}_2$  depletion. The potential at which this peak occurs,  $V_{\text{pr}}$ , is a measure of the catalytic activity. A second measure is obtained by rotating the electrode at 1500 rpm, correcting the total current for the capacitive current and for limitation by  $\text{O}_2$  diffusion in the electrolyte according to the Koutecky–Levich equation. These two measures of the activity are reliable (supplementary information of Ref. [23]). In the present work, the kinetic current density (in  $\text{A g}^{-1}$  of catalytic powder) at 0.5 V versus SCE is used in the figures. The  $V_{\text{pr}}$  values are reported in Table 1 in order to allow the reader to compare the present activities with older ones reported by our laboratory. Next, the  $\text{H}_2\text{O}_2$  yield is measured with the rotating ring disk electrode. Before each measurement, the Pt ring is cleaned by sweeping its potential between  $-0.3$  and  $1.1$  V versus SCE at 50  $\text{mV s}^{-1}$  for about 5 min. For the measurement, the disk potential is swept between  $-0.3$  and  $0.8$  V versus SCE at 2  $\text{mV s}^{-1}$  and the disk-ring is rotated at 200 rpm. Meanwhile, the ring potential is held at 1.1 V versus SCE. The disk current measured under  $\text{O}_2$  is corrected by retrieving the current recorded

Table 1  
Synthesis parameters for the catalysts

Metal content before heat-treatment (targeted) (wt.%)	Time of heat-treatment at 950 °C in $\text{NH}_3$ (min)	Weight loss percentage of carbon (wt.%)	Metal content after heat-treatment (measured by neutron activation) (wt.%)	Catalytic activity, $V_{\text{pr}}$ (mV vs. SCE)
Initial carbon black				
0	15	36.7	0.004 Fe, 0.0002 Co	162
Iron-based catalysts				
0.005	15	32.8	0.009	271
0.01	15	31.7	0.013	288
0.02	15	31.1	0.026	370
0.05	15	30.0	0.064	440
0.1	16	32.2	0.12	445
0.2	20	34.6	0.24	445
0.4	25	34.2	0.55	459
0.8	50	37.5	1.10	466
2.0	80	29.1	2.70	221
Cobalt-based catalysts				
0.005	15	30.6	0.0051	293
0.01	15	32.6	0.0093	347
0.02	15	33.2	0.015	332
0.05	15	30.6	0.057	379
0.1	15	30.6	0.094	385
0.2	15	28.3	0.20	394
0.4	19	31.7	0.37	406
0.8	22	34.2	0.87	410
1.0	20	36.4	1.12	263
1.5	18	31.3	1.73	180
2.0	20	33.3	2.40	334
5.0	18	35.5	6.90	191

under  $N_2$ . The  $H_2O_2$  yield reported is the one read at 0 V versus SCE during the first potential scan, which tends to represent the maximum yield over the range  $-0.3$  to  $0.8$  V versus SCE. It is calculated according to Eqs. (2) and (3) [36,37]:

$$\% H_2O_2 = 100 \times \frac{4 - n}{2} \quad (2)$$

where  $n$ , the apparent number of electrons transferred during ORR, is calculated according to

$$n = \frac{4I_d}{I_d + (I_r/N)} \quad (3)$$

where  $I_d$ ,  $I_r$ , and  $N$  are the disk current, ring current and ring collection efficiency, respectively.

### 2.3. Activity at 80 °C: fuel cell experiments

Membrane electrode assemblies are prepared using a Nafion 117 membrane, commercial anodes (E-TEK ELAT,  $0.35 \text{ mg Pt cm}^{-2}$ ) and cathodes made of catalyst inks deposited onto commercial electrodes (E-TEK ELAT). The formula for the cathode ink is: 10 mg of catalyst/217  $\mu\text{L}$  of Nafion solution 5 wt.%/272  $\mu\text{L}$  ethanol/136  $\mu\text{L}$  water. This formula yields a Nafion to catalyst mass ratio of 1 in the dry cathode. The ink is mixed under ultrasonic agitation for 1 h. A 71- $\mu\text{L}$  aliquot is deposited on an ELAT electrode of area  $1.14 \text{ cm}^2$ . The cathode is then dried and weighed, and the anode and cathode are hot-pressed against a Nafion 117 membrane. This procedure yields a catalyst loading at the cathode of  $1 \text{ mg cm}^{-2} \pm 10\%$  (mass of carbon + metal). The fuel cell temperature is 80 °C and the humidifier's is 105–110 °C. Humidified  $H_2$  and  $O_2$  are fed in the cell at a pressure of 2 bar absolute each, resulting in an absolute pressure of 1.5 bar each ( $p_{H_2O \text{ sat}} = 0.5 \text{ bar}$  at 80 °C). The polarization curve is recorded at a scan rate of  $0.5 \text{ mV s}^{-1}$  after a break-in at 0 V for 1 h. The cell resistance is measured by impedance spectroscopy at open circuit after the polarization curve. It is typically  $0.2 \Omega \text{ cm}^2$ .

### 2.4. Determination of elemental surface and bulk concentrations

X-ray photoelectron spectroscopy is performed with a VG Escalab 200i instrument using the Al  $K\alpha$  line (1486.6 eV). Narrow scans are recorded for the  $C_{1s}$  and  $N_{1s}$  core levels. The bulk concentration of metal in the catalysts (after heat-treatment) is determined by neutron activation analysis at the École Polytechnique de Montréal. The error on the measurement is usually  $\pm 5\%$ , but slightly higher for the lowest Fe loadings.

### 2.5. Note

In the text and in all figures, data given per gram of catalyst (e.g.  $\text{m}^2 \text{ g}^{-1}$  or  $\text{A g}^{-1}$ ) means per gram of the catalytic powder (including metal, carbon and nitrogen).

## 3. Results and discussion

### 3.1. Measurements at room temperature in $H_2SO_4$ solution of pH 1

#### 3.1.1. Conditions for a correct measurement of the turn-over frequency

The metal loading on carbon was spanned from 0.005 to 5 wt.%. As already mentioned in Section 1, in order to study the sole effect of metal loading on the ORR activity, it is extremely important that the compared catalysts contain a same amount of micropores. It has been recently demonstrated that the micropore surface area controls the activity of catalysts prepared from iron acetate and with a metal loading of 0.2 wt.% [23]. It is also known, from Fig. 2B in the same study, that the rate of carbon gasification by  $NH_3$  is slowed down when the Fe loading is increased. This effect is due to the decomposition reaction on metallic iron of some of the  $NH_3$  into  $N_2$  and  $H_2$ . Thus, heat-treating all catalysts in  $NH_3$  for a unique duration would result in various weight loss percentages of carbon, and therefore in various micropore surface areas. This would be a poor experimental strategy: the true relation between the metal content and the activity for the ORR would be skewed by the change in the catalyst microstructure. Here instead, the duration of heat-treatment was tuned with respect to the metal loading in order to keep the weight loss percentage of carbon constant (Table 1). The targeted weight loss percentage was 30–35 wt.%, which corresponds to the point at which the micropore area is maximized for the present furnace black [23]. It is then verified if holding the weight loss percentage constant actually results in a constant micropore surface area (Fig. 1). This proves correct in the range 0–1 wt.% of Fe or Co. At higher metal loading, the micropore area decreases (Fig. 1), even for a constant weight loss of carbon (Table 1). This effect can also be measured, in a simpler manner, by looking at the capacitive current (measured in  $H_2SO_4$  of pH 1 at 0.7 V versus SCE, where no Faradaic reaction occurs) of the catalysts (Fig. 2). Since the micropore

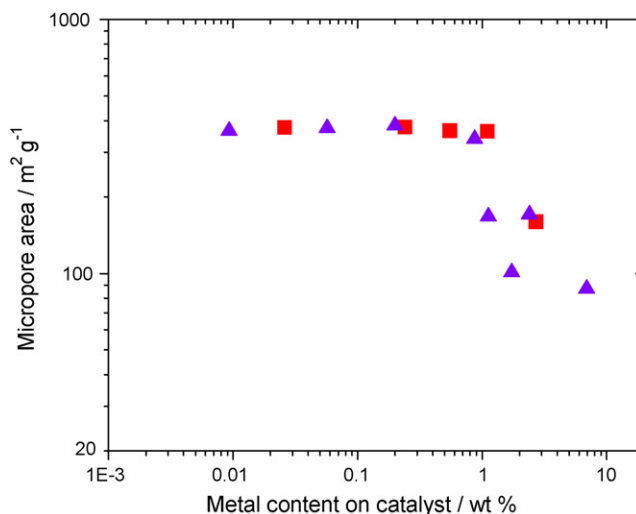


Fig. 1. Micropore specific area against metal content for (■) Fe-based and (▲) Co-based catalysts. Area is given in  $\text{m}^2/\text{g}$  of catalyst (carbon + metal).



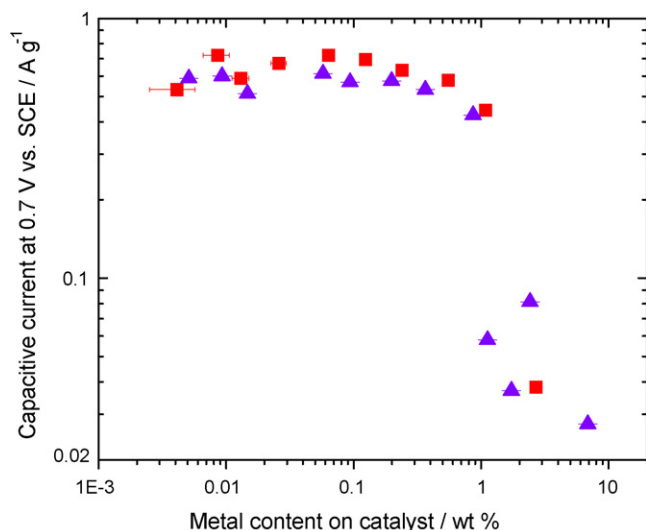


Fig. 2. Capacitive current against metal content for (■) Fe-based and (▲) Co-based catalysts. Measured in H<sub>2</sub>SO<sub>4</sub> pH 1, room temperature,  $p_{O_2}$  = 1 atm absolute.

area decreases at high metal loading, then the total BET area decreases too and this yields a decreasing capacitive current. The conclusion is that only the catalysts with a metal content below the threshold value (1 wt.% for Fe or Co) can be used to investigate the average turn-over frequency of the active sites. It must also be noted that the metal content before and after the heat-treatment has changed (Table 1). A concentration effect arises from the carbon gasification because metal atoms do not form volatile compounds during heat-treatment in NH<sub>3</sub>. It is therefore important to measure accurately the metal content after the heat-treatment. This was done by neutron activation analysis. It is the post-heat-treatment content that is used in all figures.

Another practical aspect that must be considered before relating the activity for the ORR to the metal content of the catalysts is the presence of native metal atoms, i.e. atoms that come not from the adsorption of metal acetate onto the carbon black but that were present in the pristine carbon black itself. The latter Fe concentration is 0.004 wt.% (first line of Table 1) while the concentration of native Co is 20 times smaller. Thus, the problem resides in these 0.004 wt.% Fe biasing slightly the ORR activity measured for the Co catalysts; at least for ultra-low Co contents. This bias is corrected by retrieving from the kinetic current at a given potential the kinetic current measured for the carbon black heat-treated alone (no metal acetate added prior to heat-treatment).

$$I_{\text{kinetic, corr}}(\text{fixed } E) = I_{\text{kinetic, measured}}(\text{fixed } E) - I_{\text{kinetic carbon HT alone}}(\text{fixed } E) \quad (4)$$

At 0.5 V versus SCE, the kinetic current measured on the carbon black heat-treated alone is 0.039 A g<sup>-1</sup> of catalyst (mass of carbon + Fe + N). For the Co catalysts, only the corrected activity will be displayed and discussed in the present paper. For the Fe catalysts, no correction for the presence of  $2 \times 10^{-4}$  wt.% Co was made.

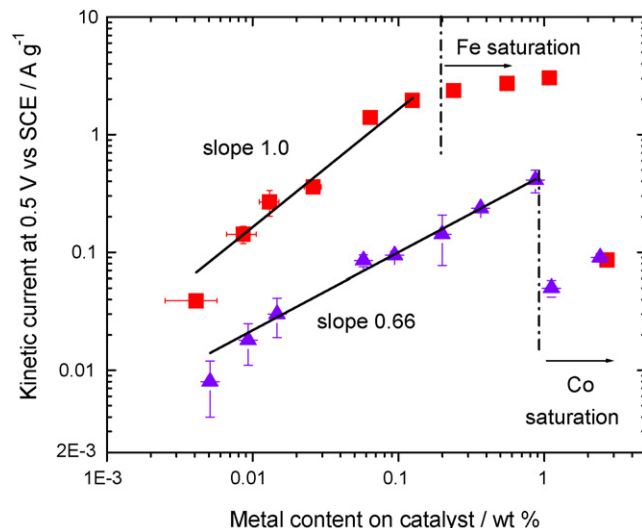


Fig. 3. Activity for O<sub>2</sub> electro-reduction at room temperature against metal content for (■) Fe-based and (▲) Co-based catalysts. The lines were obtained by fitting a law of the type  $y = ax^b$  (Eq. (5)). Measured in H<sub>2</sub>SO<sub>4</sub> pH 1, room temperature,  $p_{O_2}$  = 1 atm absolute. Current density is given in A g<sup>-1</sup> of catalytic powder (carbon + metal).

Once the above experimental traps avoided, the activity of such catalysts can be meaningfully plotted as a function of their metal concentration. Fig. 3 shows, in a log–log plane, how the activity for the ORR (in A g<sup>-1</sup> of catalyst at 0.5 V versus SCE) varies with the Fe or Co concentration. At low metal content ( $\leq 0.2$  wt.% for Fe and  $\leq 1$  wt.% for Co) the activity increases with increasing metal content. This means that, in that region, neither the N content nor the micropore specific area of the catalysts limits their activity; only the metal content limits the activity. The Tafel slope, estimated from the E–log  $i$  curves shown in Fig. 4, is 70–80 and 60–70 mV per decade for the Fe and Co catalysts, respectively. In Fig. 3, the maximum activity

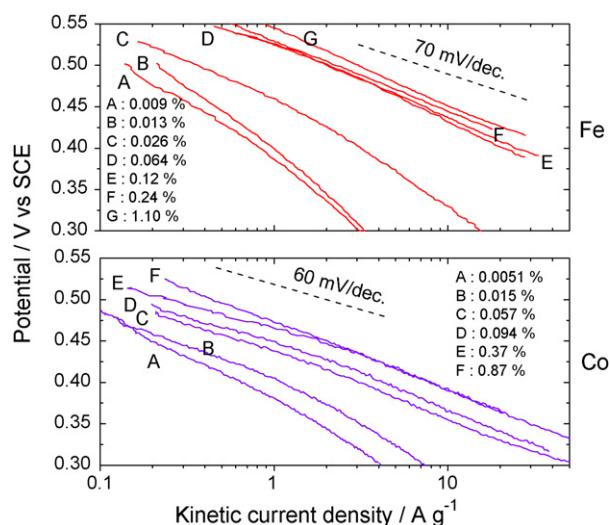


Fig. 4. RDE-polarisation curves in H<sub>2</sub>SO<sub>4</sub> solution of catalysts with various metal loadings in wt.%. Upper panel: Fe catalysts; lower panel: Co catalysts. The current has been corrected for (i) double layer current and (ii) for O<sub>2</sub> diffusion limitation in the solution. Measured at pH 1, room temperature, rotation rate of 1500 rpm and potential sweep rate of 10 mV s<sup>-1</sup>.

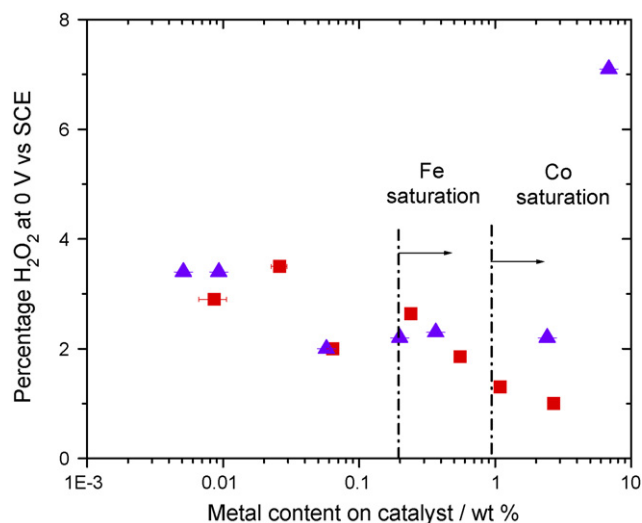


Fig. 5. Selectivity for O<sub>2</sub> electro-reduction at room temperature against metal content for (■) Fe-based and (▲) Co-based catalysts. Measured in H<sub>2</sub>SO<sub>4</sub> pH 1, room temperature,  $p_{\text{O}_2} = 1$  atm absolute.

reached by the Fe catalysts is larger than that obtained by the Co catalysts, which is in accordance with a previous study [38]. At the threshold metal content (dashed vertical lines) the activity levels off and, upon larger metal contents (>1 wt.% for Fe and Co), even decreases dramatically by one to two decades. For example, the activity of the 6.9 wt.% Co catalyst is as poor as that of the carbon heat-treated with no addition of metal (Table 1:  $V_{\text{pr}}$  of 191 and 162 mV versus SCE, respectively). The main explanation for this is the drop in micropore area (Fig. 1). The surface concentration of N atoms was 3–4 at.% for all Fe catalysts and 2–3 at.% for all Co catalysts and was about constant with metal loading. Thus, the N content cannot explain the activity drop. In summary, a first difference is unravelled between the Fe catalysts and the Co ones: the threshold content at which the metal atoms saturate the carbon support is about 0.2 wt.% for Fe against about 1 wt.% for Co; for this carbon black.

Fig. 5 depicts the change of peroxide production with the metal content of the catalysts. Only a slight decrease of the H<sub>2</sub>O<sub>2</sub> yield from about 4 to 1.5% is observed when the Fe or Co content is increased from 0.005 to 1 wt.%. This oxygen reduction mechanism of almost four-electrons for all catalysts indicates that the nature of the catalytic sites is unchanged with the metal loading. Only the site density seems to change with the metal content. However, it is believed that this apparent four-electrons reduction of O<sub>2</sub> is mainly a 2 + 2 electron reduction; the peroxide generated by the first 2e reduction on one catalytic site being able to be further reduced by another two electrons on another catalytic site in the catalyst film. This could explain why increasing the site density decreases slightly the peroxide yield, simply by increasing the probability for a peroxide molecule to meet another catalytic site on its way out of the catalytic film.

It is to be noted that Fe and Co catalysts of this study are characterized by a similar and quite low peroxide yield (<4% in Fig. 5). Previous works reported higher peroxide yields for Co catalysts [39–41]. As far as the work performed by our group is concerned, previous studies on Co catalysts reported a strong

influence of the carbon black support on the peroxide yield [41]. The latter could reach at 0 V versus SCE (i) values as high as 80% H<sub>2</sub>O<sub>2</sub> for catalysts made with Black Pearls and with a developmental high specific area graphite labeled HS300, and (ii) values as low as 15% H<sub>2</sub>O<sub>2</sub> for catalysts made with a developmental carbon black from Sid Richardson Carbon Corporation, doped with nitrogen in its bulk. This carbon was labelled RC1 in Ref. [41]. In the latter work, the % H<sub>2</sub>O<sub>2</sub> decreased with increased nitrogen concentration at the surface of the catalysts. The low % H<sub>2</sub>O<sub>2</sub> values measured for the catalysts prepared for this study may be understood in terms of nitrogen content as well. Indeed, high values of 2–3 at.% of nitrogen were measured for the Co-based catalysts depicted in Fig. 5, in agreement with the low yield of peroxide (<4%) reported for the Co-based catalysts in that figure. % H<sub>2</sub>O<sub>2</sub> < 10% were also found by other groups for Co catalysts [42,43].

### 3.1.2. Analysis of the increase in ORR activity at low metal content

In this section the catalytic activity in the region where the catalysts are not saturated in metal atoms (left handside of the vertical dashed lines in Fig. 3) is analyzed in more detail. If one assumes that, below the threshold metal content, each metal atom forms one active site and that the activity is proportional to the number of active sites; then the mass activity ( $\text{A g}^{-1}$  of catalytic powder at fixed potential) against the metal content in a log–log plane should display a slope of unity. The experimental data in the metal-unsaturated region were fitted by straight lines (Fig. 3) yielding the following empirical relations between the mass activity and the metal content:

$$I_{k,\text{Fe}}(0.5 \text{ V versus SCE}) = 16.4c_{\text{Fe}},$$

$$I_{k,\text{Co}}(0.5 \text{ V versus SCE}) = 0.46c_{\text{Co}}^{0.66} \quad (5)$$

where  $I_k$  is the kinetic current in  $\text{A g}^{-1}$  of catalyst (mass of C + metal) and  $c$  is the metal loading, in weight percentage. The error on the pre-exponential or exponential factor is 10%. The same analysis may be performed at other potentials with similar results for the exponential factors. So, a second difference is unravelled between the Fe catalysts and the Co ones: the former see their catalytic activity increase proportionally with the Fe content in the region 0–0.2 wt.% while the latter see their catalytic activity increase about as the square root of the Co content in the region 0–1 wt.%.

For the Fe catalysts, the linear increase in activity in the region 0–0.2 wt.% metal content is easily explainable if all Fe atoms form active sites during the heat-treatment. This result is in accordance with previous experimental results obtained by time-of-flight secondary-ion mass spectroscopy (time-of-flight SIMS) [18,33]. A family of catalysts synthesized in conditions not too different from those used in the present study (0.2 wt.% Fe adsorbed on an N-rich carbon support; then pyrolyzed in Ar/H<sub>2</sub> at various temperatures) was characterized by time-of-flight SIMS and by electrochemical methods [33]. It was shown that the activity for the ORR correlated well with the time-of-flight SIMS intensity of the family of ions labelled  $\text{FeN}_2\text{C}_y^+$ , and especially well with the ion  $\text{FeN}_2\text{C}_4^+$ . The latter ion could

account, for the most active catalysts, for up to 80% of the time-of-flight SIMS signal summed on all  $\text{FeN}_x\text{C}_y^+$  ions. These previous time-of-flight SIMS results say that, at 0.2 wt.% Fe content, and under heat-treatment conditions in which the activity is maximum (properly chosen combination of carbon support, time and duration of heat-treatment), a majority of Fe atoms are involved in a first active site, labelled  $\text{FeN}_2/\text{C}$  in Ref. [33]. The remaining Fe ions, about 20%, are involved in a second catalytic site labelled  $\text{FeN}_4/\text{C}$  in the same work. These catalytic sites are also expected to be present in about the same proportions in the present work since similar synthesis conditions were applied. Thus, the turn-over frequency measured in the present work represents an average of the turn-over frequency of the individual catalytic sites  $\text{FeN}_2/\text{C}$  and  $\text{FeN}_4/\text{C}$ .

Another possibility exists that would also explain the linear increase in activity with Fe content observed for Fe loadings <0.2 wt.%. Possibly, only a fraction of Fe atoms could form active sites for the ORR, provided that this fraction does not change with the metal loading. This hypothesis is however contradicted by the apparent lack of Fe crystalline phases for Fe loadings <0.2 wt.%, as explained now. Table 1 reports the time of heat-treatment at 950 °C in  $\text{NH}_3$  necessary to reach a constant weight loss of 30–35% for various Fe loadings on the catalysts. This time must be increased a lot for loadings >0.2 wt.%. This may be understood in terms of dissociation of some  $\text{NH}_3$  in the catalyst bed into  $\text{N}_2$  and  $\text{H}_2$ ; a reaction known to be catalyzed at the Fe surface [44–46]. This reasoning implies that, for Fe loadings >0.2 wt.%, some iron precursor forms metallic iron particles. On the other hand, for loadings <0.2 wt.%, no metallic Fe exists since the duration of heat-treatment remains constant at 15–16 min. As a consequence, all Fe atoms in the latter range of Fe contents are believed to form iron ions in the catalytic sites of the ORR.

The behaviour of the catalytic activity against metal content of the Co catalysts is now discussed (Fig. 3). In contrast to the Fe catalysts, for the Co catalysts the ORR activity increases about as the square root of the metal content (region 0–1 wt.%). It has been proposed by some authors that the Co active site consists of two Co atoms instead of only one [42,47]. However, such a hypothesis should result in an activity increasing faster than linearly with Co content (meaning a slope >1 in a log–log plane, Fig. 3). The opposite is observed here. Possibly, Co is able to form several species, among which only one catalyzes the ORR. If the fraction of the Co species active for the ORR to the total Co species decreases with increasing Co content, then this could give rise to an increase of the ORR activity with Co content being less than proportional. Another possibility is that some inactive Co species agglomerate onto, or somehow render inactive, the Co species catalyzing the ORR. The latter hypothesis could explain why at low Co content (<0.01 wt.%) activities for the Fe and Co catalysts get closer and also why the threshold metal content is higher for the Co catalysts than for the Fe ones (1 wt.% against 0.2). The assumption that only a minor part of all Co atoms are active for the ORR, and this even in the region of 0–1 wt.% Co, is also reinforced by recent time-of-flight SIMS measurements on similar Co catalysts [34]. In contrast to measurements on Fe catalysts [33] where the

signal of a single ion,  $\text{FeN}_2\text{C}_4^+$ , accounted for up to 80% of all  $\text{FeN}_x\text{C}_y^+$  ions, measurements on the Co catalysts did not reveal any ion showing a particularly strong signal [34]. All four families of ions ( $\text{CoNC}_y^+$ ,  $\text{CoN}_2\text{C}_y^+$ ,  $\text{CoN}_3\text{C}_y^+$ ,  $\text{CoN}_4\text{C}_y^+$ ) represented each about 10–30% of the total signal summed on all  $\text{CoN}_x\text{C}_y^+$  ions. Therefore, it is conceivable that only one of these families of  $\text{CoN}_x\text{C}_y^+$  ions originates from the ORR active sites, and that, consequently, only a fraction of the Co atoms is found in active sites for the ORR.

Last, it is not surprising to see that, unlike for the Fe catalysts, the time of heat-treatment to reach 30–35 wt.% loss is almost constant with the Co loading (Table 1). Indeed, since the famous screening experiments performed almost 100 years ago by Haber and Bosh, it is known that the best metals to catalyze the synthesis of  $\text{NH}_3$ , and also therefore its decomposition, are Ru and Fe [44–46].

A practical consequence of this section is that it is not possible to determine the turn-over frequency of the Co site because the activity of Co catalysts does not increase linearly with metal content (Eq. (5)). In contrast, for the Fe catalysts, the linear relation between activity and metal content observed between 0 and 0.2 wt.% loading enables us to determine now the average turn-over frequency of the Fe/N/C catalytic site at room temperature.

### 3.1.3. Average turn-over frequency (ATF) at room temperature of the Fe/N/C site

Since the kinetic current measured at 0.5 V versus SCE,  $I_{k,\text{Fe}}$ , increases linearly with the iron concentration,  $c_{\text{Fe}}$ , in Eq. (5), it is possible to calculate, at that voltage, the average turn-over frequency, ATF, of a single catalytic site. In order to do so, it is assumed that all Fe atoms are coordinated in active sites and that each active site hosts only one Fe atom. Then the theoretical relation between the kinetic current, the metal content and the ATF is

$$I_k(\text{fixed } E) = \frac{c_{\text{Fe}}}{100} \frac{N_a}{M_{\text{Fe}}} \text{ATF}(\text{fixed } E) \times e = \text{SD ATF}(\text{fixed } E) \times e \quad (6)$$

where  $I_k$  is the kinetic current ( $\text{A g}^{-1}$ ),  $c_{\text{Fe}}$  is the Fe loading (wt.%),  $N_a$  is Avogadro's number ( $6.02 \times 10^{23}$ ),  $M_{\text{Fe}}$  is the molar mass of Fe ( $55.8 \text{ g mol}^{-1}$ ) and  $e$  is the electric charge of a single electron ( $1.6 \times 10^{-19} \text{ C}$ ). In Eq. (6), the parameter group before ATF represents the site density, SD (active sites  $\text{g}^{-1}$ ). The ATF can be calculated equating Eq. (5) for Fe and Eq. (6). This yields  $\text{ATF}(0.5 \text{ V versus SCE}) = 0.95 \text{ e}^{-1} \text{ site}^{-1} \text{ s}^{-1}$ .

In order to extrapolate this value to the reference potential of 0.8 V versus SHE chosen in [3], the offset of 59 mV between 0.5 V versus SCE and 0.8 V versus SHE has to be taken into account. The ATF can be corrected for this offset according to a Tafel equation:

$$\begin{aligned} \text{ATF}(0.8 \text{ V versus SHE}) \\ &= \text{ATF}(0.5 \text{ V versus SCE}) \\ &\times \exp\left(\frac{-59}{70} \ln(10)\right) \approx 0.14 \text{ e}^{-1} \text{ site}^{-1} \text{ s}^{-1} \end{aligned} \quad (7)$$

Table 2

Average turn-over frequency, site density and volumetric activity at 0.8 V vs. SHE and under absolute O<sub>2</sub> pressure of 1 bar

	<i>T</i> (°C)	ATF (e <sup>−</sup> site <sup>−1</sup> s <sup>−1</sup> )	SD <sub>v</sub> (sites cm <sup>−3</sup> )	<i>I</i> <sub>k,v</sub> (A cm <sup>−3</sup> )
47 wt.% Pt/C reference	80	25	3.2 × 10 <sup>20</sup>	1300
Non-Pt-group metal catalyst target	80	2.5	3.2 × 10 <sup>20</sup>	130
0.06 wt.% Fe	80	0.38	2.6 × 10 <sup>18</sup>	0.16
0.13 wt.% Fe	80	0.35, 0.31	5.6 × 10 <sup>18</sup>	0.31, 0.28
0.30 wt.% Fe	80	0.40	12.9 × 10 <sup>18</sup>	0.82
0.87 wt.% Co	80	–	–	0.04
Fe catalysts range 0–0.25 wt.%	20	0.14	–	–

A Tafel slope of 70 mV per decade was taken, as experimentally measured (Fig. 4). The value 0.14 e<sup>−</sup> site<sup>−1</sup> s<sup>−1</sup> represents the average turn-over frequency at 0.8 V versus SCE in the range of 0–0.25 wt.% metal. If Tafel slopes of 60 and 80 mV per decade were assumed instead, ATF values of 0.10 and 0.17 would be found, respectively, giving thus an idea of the error in the value given in Eq. (7). This value is reported in Table 2.

### 3.2. Measurements in fuel cell at 80 °C

#### 3.2.1. Determination of current densities at 0.8 V

In order to measure activity parameters at 80 °C in PEFC, three Fe catalysts (0.06, 0.13 and 0.30 wt.%) and one Co catalyst (0.87 wt.%) were chosen. For Fe, these catalysts stand in the linear region (Fig. 3) with 0.30 wt.% being close to, or slightly above, the metal saturation. These three Fe catalysts were re-synthesized especially for the fuel cell tests, thus their exact Fe content is not found in Table 1 but is given here. The 0.87 wt.% Co catalyst represents the most active Co catalyst. The iR-corrected polarisation curves for these catalysts as well as for a commercial Pt Gore MEA are shown in Fig. 6. The straight Tafel slope observed for the Pt Gore MEA up to 1.5 A g<sup>−1</sup> (corre-

sponding, for 0.7 mg of Pt + C cm<sup>−2</sup>, to 1 A cm<sup>−2</sup>) proves that the experimental set-up performs well. The departure from the Tafel law for the non-noble catalysts at currents larger than 30 A g<sup>−1</sup> must thus be due to non-optimized cathode structure. For the 0.87 wt.% Co catalyst, the polarization curve extrapolated from 0.77 to 0.8 V in conditions of Fig. 6 gives a current density of 0.15 A g<sup>−1</sup> at 0.8 V. For the Fe-based catalysts, the measured current densities at 0.8 V are 0.61, 1.17 and 3.08 A g<sup>−1</sup> with 0.06, 0.13 and 0.30 wt.% Fe, respectively. Moreover, the fuel cell experiment was repeated for the 0.13 wt.% Fe catalyst to verify reproducibility. The latter is good as it may be seen by comparing the two values in Table 2 for 0.13 wt.% Fe.

#### 3.2.2. Calculation of activity, ATF and site density of the 0.06 wt.% Fe catalyst in reference conditions

From the reading of the current density at 0.8 V (assumed to represent 0.8 V versus SHE, losses at the anode being negligible with pure H<sub>2</sub>) the derivation of values for the site density and average turn-over frequency (ATF) is now detailed for the catalyst with 0.06 wt.% Fe. From this example, it will be easily understood how the calculation is applied to the two other catalysts.

- Assuming that all Fe atoms form active sites at such a low content, the site density SD (sites per gram of catalyst) is equal to  $c_{\text{Fe}}/100 \times N_{\text{a}}/M_{\text{Fe}}$  (Eq. (6)) with  $c_{\text{Fe}} = 0.06$ .

In Ref. [3] the site density and activity were given per cm<sup>3</sup> of electrode; assuming a density of 0.4 g of carbon per cm<sup>3</sup> in the porous electrode. The site density defined as such, SD<sub>v</sub>, is equal to 0.4 SD. This gives SD<sub>v</sub> = 2.6 × 10<sup>18</sup> sites cm<sup>−3</sup> for 0.06 wt.% Fe.

- The kinetic current, *I*<sub>k</sub>, read at 0.8 V versus SHE is 0.61 A g<sup>−1</sup> of catalyst (carbon plus metal) (Fig. 6). As above, this yields a current per electrode volume *I*<sub>k,v</sub> = 0.4*I*<sub>k</sub>. Next, a correction must be made for the oxygen pressure which is 1.5 bar absolute in Fig. 6 against 1 bar absolute in reference conditions. Then *I*<sub>k,v</sub> in reference conditions is 0.4*I*<sub>k</sub>/1.5 = 0.16 A cm<sup>−3</sup>.
- The ATF in reference conditions is equal to  $I_{\text{k}}/(\text{SD e}) = I_{\text{k,v}}/(\text{SD}_v \text{ e})$ . Thus ATF = 0.16/(2.6 × 10<sup>18</sup> × 1.6 × 10<sup>−19</sup>) = 0.38 e<sup>−</sup> site<sup>−1</sup> s<sup>−1</sup>.

These values, as well as the ones obtained for the two other Fe catalysts and for the Co catalyst, are gathered in Table 2 where Pt reference data and non-noble target data from [3] are also found. The ATF value obtained for the three Fe catalysts

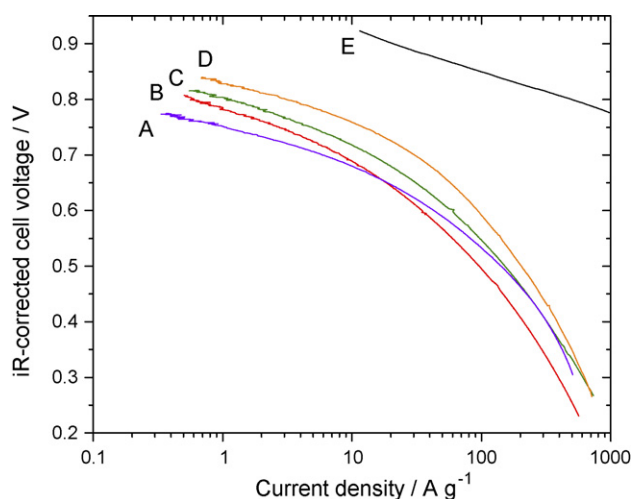


Fig. 6. iR-free fuel cell polarisation curves at 80 °C. (A) 0.87 wt.% Co; (B) 0.06 wt.% Fe (nominal 0.05 wt.%); (C) 0.13 wt.% Fe (nominal 0.1 wt.% Fe); (D) 0.30 wt.% Fe (nominal 0.2 wt.% Fe); (E) Commercial Gore 5510 MEA, 0.3 mg Pt cm<sup>−2</sup> and 45 wt.% Pt/C. H<sub>2</sub> and O<sub>2</sub> absolute pressures of 1.5 bar. The current density is in A g<sup>−1</sup> of catalyst (carbon + metal). The catalyst cathode loading is 1 mg cm<sup>−2</sup> ± 10% for the non-noble catalysts. Thus the values in A g<sup>−1</sup> are in this case almost equivalent to mA cm<sup>−2</sup>.



is fairly constant, meaning that all Fe atoms form active sites at these metal loadings or, at least, that the utilization is equal for these three catalysts. The ATF value for the Fe/N/C site in reference conditions is  $0.36 \pm 0.03 \text{ e}^{-1} \text{ site}^{-1} \text{ s}^{-1}$ . It falls in-between the wide interval of 0.02–1.7 found in [3] but is very close to the estimation of  $0.4 \text{ e}^{-1} \text{ site}^{-1} \text{ s}^{-1}$  made previously by us from a single PEFC measurement [35].

For the Co catalyst, neither the ATF nor the SD can be calculated because the Co catalysts never show a linear increase of activity with metal content (Fig. 3 and Eq. (5)).

### 3.2.3. Is the target for automotive application reachable by such non-noble catalysts?

The volumetric activity in PEFC conditions at 80 °C of the best Fe catalyst of this study is 159 times below the target for non-noble catalysts (Table 2, last column). The volumetric activity is the product of the volumetric site density,  $\text{SD}_V$ , with the average turn-over frequency, ATF. The  $\text{SD}_V$  is a factor  $\sim 25$  below the target and the ATF a factor  $\sim 7$  below the target. Thus, either one or both kinetic parameters must be increased to come closer to the target.

The ATF should be a parameter characteristic of the site, so if the sites are unchanged, this parameter cannot be improved. Thus, for the non-noble catalysts synthesized in the conditions of the present study, all improvements have to come from  $\text{SD}_V$ . In order to estimate the possibility of improvement of this parameter, one must think of how much Fe loading is theoretically possible. The active sites are believed to be made of Fe (Co) bound to at least four N atoms and to an undetermined number of C and N atoms from the C support. Molecules like phthalocyanine or porphyrin contain at least 24 or 40 atoms of C + N, respectively. Assuming that the active site cannot be made smaller than a phthalocyanine or a porphyrin molecule, an equivalent upper Fe concentration of 11–19 wt.% could theoretically be reached. Compared to the present utilizable Fe loading (about 0.3 wt.%), this represents a maximum possible improvement in  $\text{SD}_V$  of a factor 30–60. This is more than what is needed to reach the  $\text{SD}_V$  target, but falls short for the target of volumetric activity if the ATF of these catalytic sites cannot be improved. The situation is still worse for the Co-based catalysts which show a mass activity a decade smaller than the Fe ones (Fig. 6). It seems that, with the present synthesis procedure, only a small fraction of the Co atoms form active sites.

## 4. Conclusions

The activity of the Fe catalysts increases proportionally with Fe content up to about 0.2 wt.% metal while the activity of the Co catalysts increases about as the square root of the Co content up to 1 wt.%. With the present synthesis conditions, for metal contents below 0.2 wt.% Fe and 1.0 wt.% Co, neither the nitrogen content nor the micropore specific surface area of the catalysts limits the ORR activity of the obtained catalysts. The metal content solely limits the activity. For metal contents above these values, the catalytic activity first levels off for Fe, then drops for both Fe and Co catalysts once the metal content is larger than 1 wt.%. This behaviour essentially reflects the full occupa-

tion of available micropores with catalytic sites below a metal content of 1 wt.%, followed by the decrease of the microporous surface area for metal contents above 1 wt.%. The other factor that might influence the activity of such catalysts, the nitrogen content, seems to be non-limiting here since it remains high and constant for all catalysts of this study.

The maximum activity reached by Fe catalysts is about a decade larger than that reached by Co catalysts. This is valid both at 20 °C in  $\text{H}_2\text{SO}_4$  solution and at 80 °C in a PEFC.

The average turn-over frequency at 0.8 V versus SHE of the Fe/N/C site is  $0.14 \pm 0.03 \text{ e}^{-1} \text{ site}^{-1} \text{ s}^{-1}$  at room temperature in a solution of sulphuric acid pH 1 saturated by pure  $\text{O}_2$  under 1 atm pressure. The average turn-over frequency at 0.8 V versus SHE of the Fe/N/C site is  $0.36 \pm 0.03 \text{ e}^{-1} \text{ site}^{-1} \text{ s}^{-1}$  at 80 °C in a PEFC under an oxygen absolute pressure of 1 bar.

## Acknowledgements

This work is supported by NSERC and General Motors of Canada. The authors are indebted to the Sid Richardson Carbon Company for providing the carbon black.

## References

- [1] M. Mathias, H. Gasteiger, R. Makharia, S. Kocha, T. Fuller, T. Xie, J. Pisco, ACS Div. Fuel Chem. 49 (2004) 471 (Preprints).
- [2] S. Mukerjee, S. Srinivasan, M.P. Soriaga, J. Mc Breen, J. Electrochem. Soc. 142 (1995) 1409.
- [3] H.A. Gasteiger, S.S. Kocha, B. Sompalli, F.T. Wagner, Appl. Catal. B: Environ. 56 (2005) 9.
- [4] K. Sasaki, Y. Mo, J.X. Wang, M. Balasubramanian, F. Uribe, J. McBreen, R.R. Adzic, Electrochim. Acta 48 (2003) 3841.
- [5] J. Zhang, F.H.B. Lima, M.H. Shao, K. Sasaki, J.X. Wang, J. Hanson, R.R. Adzic, J. Phys. Chem. B 109 (2005) 22701.
- [6] V.S. Bagotzky, M.R. Tarasevich, K.A. Radyushkina, O.E. Levina, S.I. Andrusyova, J. Power Sources 2 (1977) 233.
- [7] R.W. Joyner, J.A.R. van Veen, W.M.H. Sachtler, J. Chem. Soc., Faraday Trans. 1 78 (1982) 1021.
- [8] B. van Wingerden, J.A.R. Van Veen, C.T.J. Mensch, J. Chem. Soc., Faraday Trans. 84 (1988) 65.
- [9] L. Zhang, C. Song, J. Zhang, H. Wang, D.P. Wilkinson, J. Electrochem. Soc. 152 (2005) A2421.
- [10] P. Bogdanoff, I. Herrmann, M. Hilgendorff, I. Dorbrandt, S. Fiechter, H. Tributsch, J. New Mater. Electrochem. Syst. 7 (2004) 85.
- [11] I. Herrmann, P. Bogdanoff, G. Schmithals, S. Fiechter, ECS Trans. 3 (2006) 211.
- [12] S. Gupta, D. Tryk, I. Bae, W. Aldred, E. Yeager, J. Appl. Electrochem. 19 (1989) 19.
- [13] D. Ohms, S. Herzog, R. Franke, V. Neumann, K. Wiesener, S. Gamburgcev, A. Kaisheva, I. Iliev, J. Power Sources 38 (1992) 327.
- [14] G. Lalande, R. Côté, D. Guay, J.P. Dodelet, L.T. Weng, P. Bertrand, Electrochim. Acta 42 (1997) 1379.
- [15] R. Côté, G. Lalande, D. Guay, J.P. Dodelet, G. Dénés, J. Electrochem. Soc. 145 (1998) 2411.
- [16] G. Faubert, R. Côté, J.P. Dodelet, M. Lefèvre, P. Bertrand, Electrochim. Acta 44 (1999) 2589.
- [17] A.L. Bouwkamp-Wijnoltz, W. Visscher, J.A.R. Van Veen, S.C. Tang, Electrochim. Acta 45 (1999) 379.
- [18] M. Lefèvre, J.P. Dodelet, P. Bertrand, J. Phys. Chem. B 104 (2000) 11238.
- [19] M. Bron, J. Radnik, M. Fieber-Erdmann, P. Bogdanoff, S. Fiechter, J. Electroanal. Chem. 535 (2002) 113.
- [20] M. Bron, S. Fiechter, P. Bogdanoff, H. Tributsch, Fuel Cells 2 (2003) 137.

- [21] F. Jaouen, S. Marcotte, J.P. Dodelet, G. Lindbergh, *J. Phys. Chem. B* 107 (2003) 1376.
- [22] M. Yuasa, A. Yamaguchi, H. Itsuki, K. Tanaka, M. Yamamoto, K. Oyaizu, *Chem. Mater.* 17 (2005) 4278.
- [23] F. Jaouen, M. Lefèvre, J.-P. Dodelet, M. Cai, *J. Phys. Chem. B* 110 (2006) 5553.
- [24] N.P. Subramanian, S.P. Kumaraguru, H. Colon-mercado, H. Km, B.N. Popov, T. Black, D.A. Chen, *J. Power Sources* 157 (2006) 56.
- [25] E.B. Easton, A. Bonakdarpour, J.R. Dahn, *Electrochem. Solid-State Lett.* 9 (2006) A463.
- [26] I. Herrmann, V. Brüser, S. Fiechter, H. Kersten, P. Bogdanoff, *J. Electrochem. Soc.* 152 (2005) A2179.
- [27] R. Bashyam, P. Zelenay, *Nature* 443 (2006) 63.
- [28] J.-P. Dodelet, Oxygen reduction in PEM fuel cell conditions: heat-treated non-precious metal–N<sub>4</sub> macrocycles and beyond, in: J. Zagal, F. Bedioui, J.-P. Dodelet (Eds.), *N<sub>4</sub>-Macrocyclic Metal Complexes: Electrocatalysis, Electrophotochemistry & Biomimetic Electroanalysis*, Springer Science + Business Media Inc., New York, 2006 (Chapter 3).
- [29] L. Zhang, J. Zhang, D.P. Wilkinson, H. Wang, *J. Power Sources* 156 (2006) 171.
- [30] U.A. Paulus, A. Wokaun, G.G. Scherer, T.J. Schmidt, V. Stamenkovic, N.M. Markovic, P.N. Ross, *Electrochim. Acta* 47 (2002) 3787.
- [31] S. Mukerjee, S. Srinivasan, *J. Electroanal. Chem.* 357 (1993) 201.
- [32] H. Wang, R. Côté, G. Faubert, D. Guay, J.P. Dodelet, *J. Phys. Chem. B* 103 (1999) 2042.
- [33] M. Lefèvre, J.-P. Dodelet, P. Bertrand, *J. Phys. Chem. B* 106 (2002) 8705.
- [34] M. Lefèvre, J.-P. Dodelet, P. Bertrand, *J. Phys. Chem. B* 109 (2005) 16718.
- [35] F. Jaouen, F. Charreteur, J.P. Dodelet, *J. Electrochem. Soc.* 153 (2006) A689.
- [36] U.A. Paulus, T.J. Schmidt, H.A. Gasteiger, R.J. Behm, *J. Electroanal. Chem.* 495 (2001) 134.
- [37] M. Lefèvre, J.P. Dodelet, *Electrochim. Acta* 48 (2003) 2749.
- [38] P. He, M. Lefèvre, G. Faubert, J.P. Dodelet, *J. New Mater. Electrochem. Syst.* 2 (1999) 243.
- [39] P. Gouérec, A. Biloul, O. Contamin, G. Scarbeck, M. Savy, J. Riga, L.T. Weng, P. Bertrand, *J. Electroanal. Chem.* 422 (1997) 61.
- [40] T. Okada, M. Gokita, M. Yusada, I. Sekine, *J. Electrochem. Soc.* 145 (1999) 815.
- [41] S. Marcotte, D. Villers, N. Guillet, L. Roué, J.P. Dodelet, *Electrochim. Acta* 50 (2004) 179.
- [42] A. Biloul, O. Contamin, G. Scarbek, M. Savy, B. Palys, J. Riga, J. Verbist, *J. Electroanal. Chem.* 365 (1994) 239.
- [43] P. Gouérec, A. Biloul, O. Contamin, G. Scarbeck, M. Savy, J.M. Barbe, R. Guillard, *J. Electroanal. Chem.* 398 (1995) 67.
- [44] J. Leppälathi, P. Simell, E. Kurkela, *Fuel Process. Technol.* 29 (1991) 43.
- [45] H. Mori, K. Asami, Y. Ohtsuka, *Energy Fuels* 10 (1996) 1022.
- [46] P. Schaaf, *Progr. Mater. Sci.* 47 (2002) 1.
- [47] A. Biloul, F. Coowar, O. Contamin, G. Scarbek, M. Savy, D. Van den Harn, J. Riga, J.J. Verbist, *J. Electroanal. Chem.* 350 (1993) 189.